Journal of Organometallic Chemistry, 473 (1994) 139–147

Synthesis and reactivity of platinum-containing heterodinuclear complexes with methyl and 1,2-bis(diphenylphosphino)ethane ligands. X-Ray crystal structure of (dpe)MePt–$FeCp(CO)_2 \cdot THF$

Atsushi Fukuoka, Takanori Sadashima, Takeshi Sugiura, Xiaosong Wu, Yuji Mizuho and Sanshiro Komiya

Department of Applied Chemistry, Tokyo University of Agriculture and Technology, 2-24-16 Nakacho, Koganei, Tokyo 184 (Japan)

(Received September 22, 1993; in revised form November 26, 1993)

Abstract

New platinum-containing heterodinuclear complexes with methyl and 1,2-bis(diphenylphosphino)ethane (dpe) ligands have been prepared by metathetical reactions of $PtMe(NO_3)$(dpe) with $Na[ML_n]$: $ML_n = MoCp(CO)_3$ (**1**); $WCp(CO)_3$ (**2**); $Mn(CO)_5$ (**3**); $FeCp(CO)_2$ (**4**); $Co(CO)_4$ (**5**). The molecular structure of (dpe)MePt–$FeCp(CO)_2 \cdot$ THF (**4** · THF) has been determined by X-ray crystallography: the geometry at Pt is square planar and the $FeCp(CO)_2$ moiety has a piano-stool type structure. Thermolysis of **4** in C_6D_6 at 70°C for 2 h gives $MeFeCp(CO)_2$ (**8**) in 30% yield, but other dinuclear complexes are thermally stable under these conditions. Methyl migration to produce **8** was accelerated by the addition of electron-deficient olefins such as acrylonitrile and fumaronitrile. From the kinetic study, a mechanism involving two pathways is proposed: one is direct thermolysis from **4** to **8**, while the other is the associative reductive elimination of **8** from the olefin-coordinated intermediate **9**.

Key words: Molybdenum; Platinum; Heterobimetallics; Iron; Tungsten; Manganese; Cobalt

1. Introduction

Heterodinuclear complexes and heterometallic clusters continue to attract interest not only as a class of models of active sites in heterogeneous bimetallic catalysts but also as potential precursors in homogeneous catalysis [1]. We have reported the synthesis of (cod)RPt–$MCp(CO)_3$ [2] and $(PPh_3)_2$(CO)(styryl)Ru–$MCp(CO)_3$ [3] via the metathetical reactions of $Na[MCp(CO)_3]$ (M = Mo, W) with PtRX(cod) (cod = 1,5-cyclooctadiene; R = alkyl, aryl; X = Cl, NO_3) or Ru(styryl)Cl(CO)$(PPh_3)_2$, and the molecular structures of (cod)PhPt–$MCp(CO)_3$ (M = Mo, W) have been determined [2b,4]. It was notable that the organic groups on Pt migrated to Mo or W on thermolysis as well as on interaction with CO, tertiary phosphines and electron-deficient olefins such as acrylonitrile. In the present work, a series of Pt-containing heterodinuclear complexes with methyl and 1,2-bis(diphenylphosphino)ethane (dpe) ligands has been prepared by similar metathetical reactions. The characterization and chemical reactivity of the new complexes are also described. During the course of our continuing investigation concerning heterodinuclear organometallic compounds, Braunstein *et al.* reported the preparation of some PPh_3 analogues, $(PPh_3)_2$MePt–ML_n [ML_n = $MoCp(CO)_3$, $WCp(CO)_3$, $Mn(CO)_5$, $Co(CO)_4$] from $PtMe(OClO_3)(PPh_3)_2$ and $Na[ML_n]$ [5].

2. Results and discussion

2.1. Synthesis and characterization of (dpe)MePt–ML_n

Reactions of $PtMe(NO_3)$(dpe), prepared *in situ* from PtMeCl(dpe) and $AgNO_3$, with excess amounts of sodium salts of carbonylmetalate anions in THF under N_2 gave new heterodinuclear complexes in fairly good yields [eqn. (1)]. These complexes were obtained as crystals by recrystallization from THF/hexane or benzene/hexane. Complexes **1–5** exhibit high air stability as solids. The melting points (dec.) of **1** and **2** are much

Correspondence to: Dr. S. Komiya.

0022-328X/94/$7.00
SSDI 0022-328X(93)24318-Y

higher than those of the cod analogues (cod)MePt–MoCp(CO)$_3$ (**6**) and (cod)MePt–WCp(CO)$_3$ (**7**); **1**, 175 vs. **6**, 116°C; and **2**, 207 vs. **7**, 105°C. Satisfactory results for elemental analyses were obtained for **1**, **3–5** and it is suggested that **4** contains a THF molecule in the crystal, as demonstrated by ^{1}H NMR spectroscopy and X-ray crystallography. The molar electric conductivities of **1–5** were quite low, suggesting that they are not ionic complexes but neutral ones. Acidolysis of **1-5** with conc. H_2SO_4 produced CH_4 in 68–98% yield, confirming the presence of methyl groups.

$$PtMe(NO_3)(dpe) + Na[ML_n] \xrightarrow[-NaNO_3]{THF} (dpe)MePt\text{–}ML_n \quad (1)$$

(1–5)

1: $ML_n = MoCp(CO)_3$

2: $ML_n = WCp(CO)_3$

3: $ML_n = Mn(CO)_5$

4: $ML_n = FeCp(CO)_2$

5: $ML_n = Co(CO)_4$

Selected ^{1}H NMR and IR data of **1–5** are summarized in Table 1. In the ^{1}H NMR spectra of the C_6D_6 solutions, resonances due to the methyl groups were observed as triplets with ^{195}Pt satellites for **1–4** and as a doublet of doublet for **5**. The triplets were derived from the accidental coincidence of ^3J(P–H) values for the methyl protons and two phosphorus nuclei of dpe. The difference in magnetic circumstances for the two P nuclei indicates that the geometry at Pt is square planar. The ^2J(Pt–H) values of Me for **1** (60 Hz) and **2** (58 Hz) are smaller than those for the cod analogues **6** and **7** (both 75 Hz) [2], implying that the *trans* influence of dpe is stronger than that of cod [6]. Cp protons in **1**, **2** and **4** appeared as singlets at 4.2–4.7 ppm. The *ortho* protons of Ph in the dpe ligands were separated as two sets of signals at 7.7–7.9 ppm, each with 4H intensity. This result shows that the two phosphorus nuclei in dpe are not magnetically equivalent because of the Me groups and the ML_n moiety *trans* to them. In comparison to **6** and **7**, the resonances for the Me and Cp protons in **1** and **2** were shifted downfield, suggesting a lower electron density at Pt and Mo (or W).

The IR spectra of **1** and **2** exhibited ν(CO) bands at approximately 1900 and 1800 cm^{-1}, whose frequencies were similar to those for Na[MoCp(CO)$_3$] and Na[WCp(CO)$_3$]. Complex **5** also gave ν(CO) bands similar to those of Na[Co(CO)$_4$]. These data suggest that the back-bonding from Mo (or W, Co) to CO is strong in **1**, **2** and **5**. Thus, the oxidation states of the metals are expected to be close to Pt^{II} and M^0 (M = Mo, W, Co), although the formal ones are counted as Pt^I and M^I. In contrast, the ν(CO) bands of **3** were shifted to higher frequencies compared to Na[Mn(CO)$_5$], implying weak back-bonding from Mn to CO. The ν(CO) frequencies of **4** (1926; 1869 cm^{-1}, KBr) were at a position intermediate between those of K[FeCp(CO)$_2$] (1871; 1794; 1783 cm^{-1}, THF) [7a] and of MeFeCp(CO)$_2$ (2005; 1945 cm^{-1}, KBr). These IR data show that the back-bonding from Fe to CO in **4** is not so strong as that in the Pt–Mo and Pt–W analogues **1** and **2**. A related chloroplatinum–iron complex (PPh$_3$)$_2$Cl-Pt–FeCp(CO)$_2$ had much higher ν(CO) frequencies (2050; 2002 cm^{-1}, Nujol) [7b] than **4**, which is probably due to the electron-withdrawing effect of the Cl ligand.

Bryndza *et al.* also reported the formation of complexes **1** and **2** from (dpe)MePtOMe and Cp(CO)$_3$MH (M = Mo, W) [8]. However, the complexes were not isolated and details of the preparation and characterization were not reported either.

2.2. Molecular structure of (dpe)MePt–FeCp(CO)$_2$ · THF (4 · THF)

Complex **4** · THF has been subjected to a single-crystal X-ray diffraction study. The crystallographic data are summarized in Table 2, selected bond distances and angles are listed in Table 3 and an ORTEP

TABLE 1. Selected ^{1}H NMR and IR data for complexes **1–5**

Complex	^{1}H NMR [a]				IR [b]
	Me			Cp	ν(CO) (cm^{-1})
	δ (ppm)	^2J(Pt–H) (Hz)	^3J(P–H) (Hz)	δ (ppm)	
(dpe)MePt–MoCp(CO)$_3$ (**1**)	1.44(t, 3H)	59.7	6.1	4.63 (s, 5H)	1907; 1795
(dpe)MePt–WCp(CO)$_3$ (**2**)	1.64 (t, 3H)	57.6	6.8	4.59 (s, 5H)	1894; 1797; 1782
(dpe)MePt–Mn(CO)$_5$ (**3**)	1.42 (t, 3H)	62.3	6.4		2038; 1946; 1905; 1866
(dpe)MePt–FeCp(CO)$_2$ (**4**)	1.59 (t, 3H)	69.5	6.6	4.25 (s, 5H)	1926; 1869
(dpe)MePt–Co(CO)$_4$ (**5**)	1.17 (dd, 3H)	57.2	7.8, 5.8		2034; 1956; 1881; 1855

[a] In C_6D_6 at room temperature.
[b] KBr disk.

TABLE 2. Crystallographic data for (dpe)MePt-FeCp(CO)$_2$ · THF

Formula	$C_{38}H_{40}O_3P_2FePt$
M (g mol^{-1})	857.6
Crystal system	triclinic
Space group	$P\bar{1}$
a(Å)	12.166(6)
b(Å)	18.002(14)
c(Å)	9.451(4)
α(°)	97.64(7)
β(°)	101.70(4)
γ(°)	114.82(5)
V(Å^3)	1783(2)
Z	2
D_{calc} (g cm^{-3})	1.60
Radiation (Å)	Mo Kα, 0.71069
μ(Mo Kα)(cm^{-1})	8.73
Temperature	room temp.
2θ(°)	$3 < 2\theta < 55$
Scan type	$2\theta/\omega$
No. of data collected	8800
No. of obs. reflections for refinement	6642($\|F_o\| > 3\sigma\|F_o\|$)
R [a]	0.0655
R_w [b]	0.0799
S	1.89
Method of phase determination	direct method

[a] $R = \Sigma[|F_o| - |F_c|]/\Sigma|F_o|$.
[b] $R_w = [\Sigma(w[|F_o| - |F_c|]^2)/\Sigma w(|F_o|)^2]^{1/2}$.

TABLE 3. Selected bond distances and angles for (dpe)MePt-FeCp(CO)$_2$ · THF

Bond distance (Å)			
Pt–Fe	2.685(1)	Pt–P(1)	2.282(2)
Pt–P(2)	2.227(2)	Pt–C(1)	2.154(8)
Fe–C(28)	2.140(9)	Fe–C(29)	2.118(9)
Fe–C(30)	2.092(9)	Fe–C(31)	2.05(1)
Fe–C(32)	2.10(1)	Fe–C(33)	1.741(8)
Fe–C(34)	1.75(1)	O(1)–C(33)	1.15(1)
O(1)–C(34)	1.15(1)		
Bond angle (°)			
Fe–Pt–P(1)	95.35(6)	Fe–Pt–C(1)	90.2(3)
P(1)–Pt–P(2)	85.92(7)	P(2)–Pt–C(1)	88.5(3)
Pt–Fe–C(33)	97.9(3)	Pt–Fe–C(34)	74.4(3)
C(33)–Fe–C(34)	92.1(4)	Fe–C(33)–O(1)	175.0(9)
Fe–C(34)–O(2)	177.4(9)		

drawing is depicted in Fig. 1. The Pt–Fe distance is 2.685(1) Å, which falls in the range of the Pt–Fe single bond distances observed in the related Pt–Fe complexes (2.5–2.8 Å) [9]. The Pt–C(1) (CH_3) distance of 2.154 (8) Å is slightly longer than those in the other Pt^{II}–Me complexes (2.08–2.12 Å) [10]. The geometry at Pt is typically square planar, and the $FeCp(CO)_2$ moiety has a piano-stool type structure. These geometrical features around both metals are consistent with the electronic configurations and oxidation states of d^8 Pt^{II} and d^8 Fe^0, as suggested by the spectroscopic results. The Pt–P(1) distance *trans* to Me is longer than the Pt–P(2) distance *trans* to Fe, reflecting a stronger *trans* influence of Me than that of $FeCp(CO)_2$.

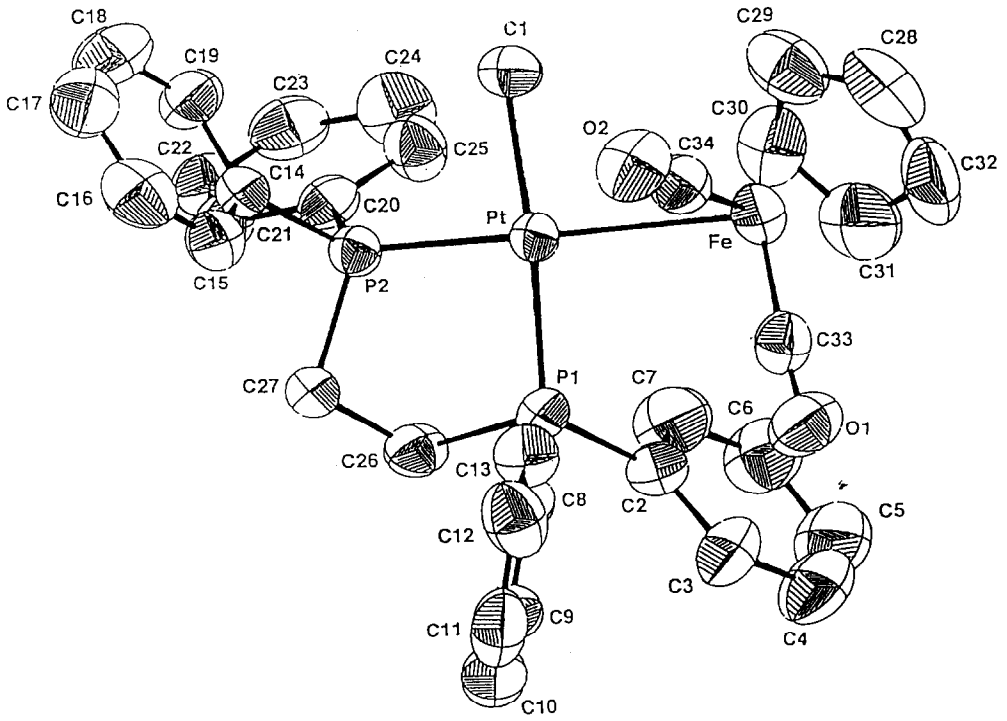

Fig. 1. ORTEP drawing of (dpe)MePt-FeCp(CO)$_2$ · THF.

For the Cp ligand, the Fe–C(31) distance of 2.05(1) Å is shorter than the other four Fe–C distances of 2.10–2.14 Å, although the latter four are almost the same values as those for related complexes such as $FeCp(CO)_2[C_6H_7(CN)_4]$ [11] and $(CO)_2CpFe(CH_2CO)ML_n$ [ML_n = NiCp(CO) and $Mn(CO)_5$] [12]. This difference in Fe–C(Cp) distances is probably due to the steric repulsion between Cp and the Ph groups of dpe. For three legs of the piano-stool, the Pt–Fe–C(34) angle of 74.4(3)° is substantially smaller than the other two angles of Pt–Fe–C(33) and C(33)–Fe–C(34) [97.9(3) and 92.1(4)°, respectively]. Thus, a weak interaction seems to exist between the C(34)–O(2) ligand and Pt. However, the Pt...C(34) distance of 2.78 Å is long for a μ-CO ligand, and the Fe–C(34) and C(34)–O(2) distances are not lengthened in comparison to Fe–C(33) and C(33)–O(1). In addition, the Fe–C(33)–O(1) and Fe–C(34)–O(2) bond angles are 175.0 and 177.4°, respectively, indicating that the CO ligands are not bent. These data suggest that the CO ligands coordinate to Fe essentially in a terminal fashion.

2.3. *Reactivity of the heterodinuclear complexes 1–5*

The reactions of **1–5** with I_2 result in cleavage of the Pt–M and Pt–Me bonds. The products and their yields are summarized in Table 4. Typically, **4** in C_6D_6 was treated with 1 equiv. I_2 for 12 h when the ^1H NMR spectrum of the solution showed the formation of (dpe)MePtI (38%), $IFeCp(CO)_2$ (25%) and MeI (11%) [eqn. (2)]. On the other hand, reaction of **4** with excess I_2 for 60 h gave MeI (71%), $IFeCp(CO)_2$ (77%) and yellow precipitates, but (dpe)MePtI was not observed in the solution. These results indicate that the iodolysis of Pt–Fe and Pt–Me bonds apparently occurs at the same time, but that the Pt–Fe bond is more easily cleaved than the Pt–Me bond. In the presence of excess I_2, the Pt–Me bond in (dpe)MePtI is further cleaved to give MeI and $(dpe)PtI_2$, the latter not being detected by ^1H NMR spectroscopy due to the low solubility in C_6D_6. Similarly, the Pt–M and Pt–Me bonds were cleaved at the same time for **1–3**. We previously demonstrated that the iodolysis of the Pt–Mo and Pt–W cod analogues **6** and **7** proceeds by a mechanism involving initial formation of an $MePt^{II}$ species which further gave MeI and PtI_2(cod) [2a]. A similar stepwise process may be operative in the present reactions, but the reactivity of the dpe derivatives **1–5** toward MeI is higher than that of **6** and **7**.

$$(dpe)MePt–FeCp(CO)_2 + I_2 \longrightarrow (dpe)MePtI + IFeCp(CO)_2 + MeI \quad (2)$$

We found previously that Pt–Mo and –W complexes **6** and **7** in C_6D_6 underwent methyl migration, *i.e.* reductive elimination of Me and $MCp(CO)_3$, to give $MeMCp(CO)_3$ in 45–73% yield after 2 h at 70°C [2b]. Accordingly, the thermolysis reactions of **1–5** have been examined under the same reaction conditions. Only **4** afforded $MeFeCp(CO)_2$ (**8**) in 30% yield [eqn. (3)], but no reaction took place with the other complexes **1–3** and **5**. Since *cis*-dialkylplatinum(II) complexes apparently do not eliminate R–R readily [13], this result shows a promotion effect of the $FeCp(CO)_2$ fragment on the reductive elimination. On the other hand, it is shown that other metal fragments such as $MoCp(CO)_3$, $WCp(CO)_3$, $Mn(CO)_5$ and $Co(CO)_4$ have a negligible effect. The lower activity of **1** and **2** than the cod analogues **6** and **7** in the thermolysis reactions probably results from a higher thermal stability, as

TABLE 4. Products and their yields in the iodolysis of (dpe)MePt–ML_n [a]

Complex	(mmol)	I_2 (equiv.)	Time (h)	(dpe)MePtI (%)	IML_n (%)	MeI (%)
(dpe)MePt–$MoCp(CO)_3$ (**1**)	0.0124	0.75	0.5	12	14	5
		1	12	41	98	39
		excess	48	0	18	56
(dpe)MePt–$WCp(CO)_3$ (**2**)	0.0190	1	12	61	62	10
		excess	12	0	< 1	67
(dpe)MePt–$Mn(CO)_5$ (**3**)	0.0161	1	3	0	0	12
		1	48	31	0	17
		excess	12	0	0	75
(dpe)MePt–$FeCp(CO)_2$ (**4**)	0.0140	1	3	30	33 [b]	9
	0.0248	1	12	38	25 [c]	11
	0.0248	excess	60	0	77	71
(dpe)MePt–$Co(CO)_4$ (**5**)	0.0192	1	12	n.d. [d]	0	35
		excess	12	n.d. [d]	0	79

[a] In C_6D_6 at room temperature.
[b] $[FeCp(CO)_2]_2$, 24%.
[c] $[FeCp(CO)_2]_2$, 36%.
[d] Not determined.

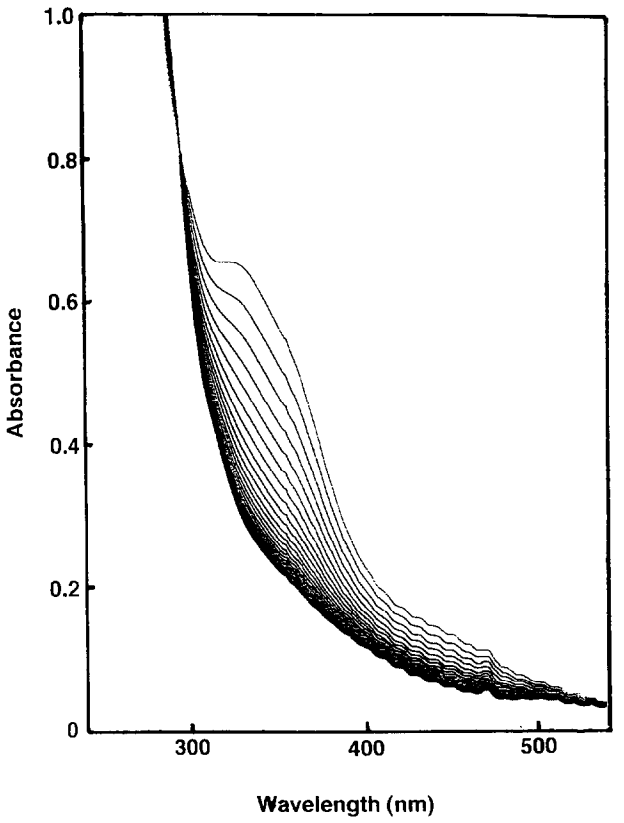

Fig. 2. UV–vis spectral changes for **4** in the presence of acrylonitrile (AN). Solvent, THF; temperature, 38.5°C; [**4**] = 8×10^{-5} M; [AN] = 7.46×10^{-2} M.

demonstrated by the higher melting points (dec.) of **1** and **2** relative to **6** and **7**, as described above.

$$\underset{(4)}{(dpe)MePt\text{–}FeCp(CO)_2} \xrightarrow{\Delta} \underset{(8)}{MeFeCp(CO)_2} \quad (3)$$

The methyl migration reactions were promoted by CO: reaction of a C_6D_6 solution of **4** with CO (1 atm) for 3 h at room temperature afforded **8** (8% yield) and $[FeCp(CO)_2]_2$ (trace), although **8** was not formed at room temperature in the absence of CO. Complex **3** gave $MeMn(CO)_5$ (11%) and $MeCOMn(CO)_5$ (27%) under the same reaction conditions. In contrast, no reaction took place with complexes **1**, **2** and **5**, even in the presence of CO.

Acceleration of methyl migration was also observed when olefins such as acrylonitrile (AN) and fumaronitrile (FN) were added. Typically, treatment of a C_6D_6 solution of **4** with 5 equiv. AN at room temperature for 2 h gave **8** in 26% yield [eqn. (4)]. The Pt product was (dpe)Pt(AN), which could be isolated in a large scale experiment. The yield of **8** increased up to 96% after 78 h, when (dpe)Pt(AN) was formed in 75% yield. This result strongly supports the suggestion that in the present methyl migration reactions the Pt product is essentially the Pt^0 complex. We suggest that acceleration is due to coordination of the π-acidic ligands to Pt, resulting in the reductive elimination of **8** [14]. No reaction was observed for **1–3** and **5** at room temperature, but **3** gave $MeMn(CO)_5$ (17%) after 1 h at 50°C.

$$\underset{(4)}{(dpe)MePt\text{–}FeCp(CO)_2} + AN \longrightarrow \underset{(8)}{(dpe)Pt(AN)} + MeFeCp(CO)_2 \quad (4)$$

2.4. Mechanism of methyl migration in (dpe)MePt–FeCp(CO)$_2$ (4)

The methyl migration in complex **4** in the presence of AN was examined in detail. In UV–vis spectroscopy,

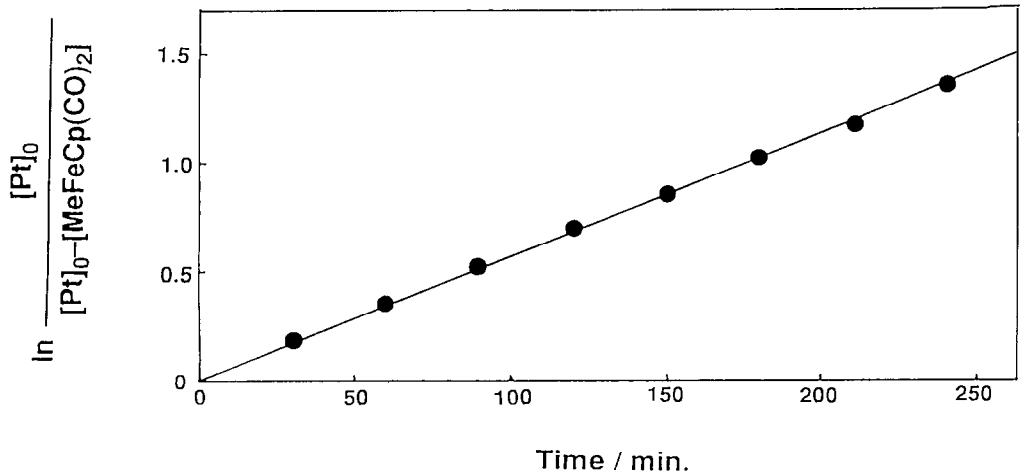

Fig. 3. First-order plot for the reaction of **4** with acrylonitrile (AN).

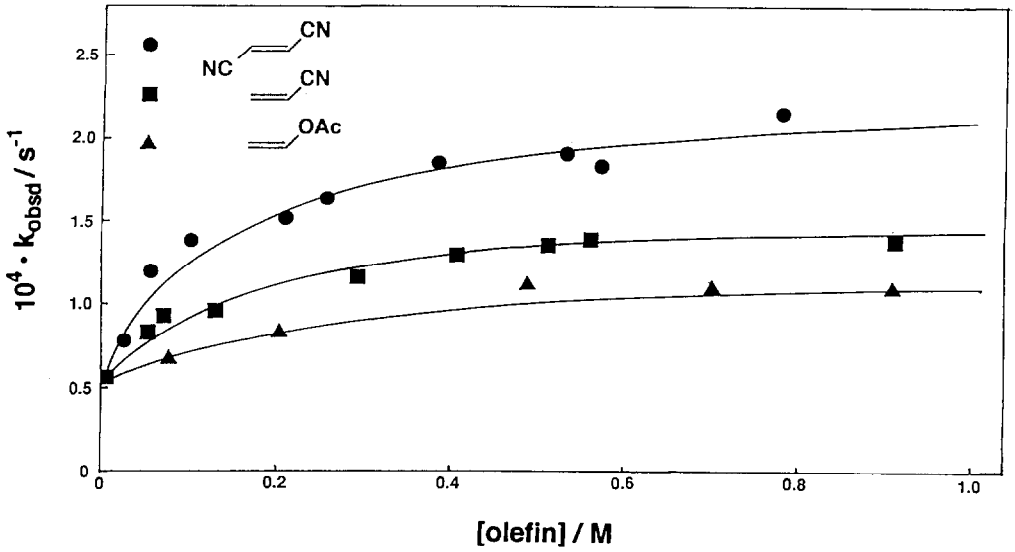

Fig. 4. Dependence of $k_{obs.}$ on the concentration of olefin.

a THF solution of **4** gave an absorption band at 322 nm which was not observed for the precursors PtMe(NO_3)(dpe) and Na[FeCp(CO)$_2$]. We postulate that the band should be ascribed to the Pt–Fe bond. Accordingly, reaction of **4** with AN was followed by UV–vis spectral changes (Fig. 2). In Fig. 2, an isosbestic point appears at 292 nm, indicating the absence of stable intermediates other than **4** and **8**. The rate of formation of **8** was obtained by monitoring the decrease in concentration of **4**, and the resulting first-order plot was a straight line (Fig. 3). From the slope of the line, a pseudo-first-order rate constant ($k_{obs.}$) was obtained (Table 5). Reactions of **4** with fumaronitrile and vinyl acetate were conducted in a similar manner. Plots of $k_{obs.}$ versus concentration for the three olefins yielded curves (Fig. 4) in which $k_{obs.}$ approached a constant value with an increase in the olefin concentration. As shown in Fig. 4, acceleration of methyl migration by the olefins occurs in the following order: fumaronitrile > acrylonitrile > vinyl acetate. This is the same order as the electron deficiency for the three olefins, as indicated by the Alfrey–Price *e* value [15]: fumaronitrile (e = 1.96) > acrylonitrile (1.20) > vinyl acetate (−0.22).

TABLE 5. Pseudo-first order rate constants for the reaction of **4** with olefin

Olefin [a]	[Olefin] (M×10)	[**4**] (M×10^5)	Temp. (°C)	k_{obs} (s^{-1}×10^4)
FN	0.284	3	37.3	0.780
	0.562	3	39.0	1.21
	1.03	4	38.2	1.38
	2.13	8	38.0	1.49
	2.58	4	38.3	1.63
	3.91	4	37.0	1.86
	5.34	6	38.8	1.91
	5.73	4	38.0	1.82
	7.84	5	38.5	2.14
AN	0.096	3	37.6	0.572
	0.518	3	38.0	0.840
	0.749	2	37.2	0.938
	1.34	3	38.0	0.953
	2.97	3	37.5	1.15
	4.13	3	39.0	1.29
	5.15	1	39.0	1.35
	5.65	1	38.1	1.39
	9.16	6	38.0	1.37
VAc	0.792	4	38.0	0.671
	2.04	4	38.2	0.817
	4.87	4	37.9	1.13
	7.02	6	38.0	1.10
	9.09	5	38.0	1.10

[a] FN = fumaronitrile; AN = acrylonitrile; VAc = vinyl acetate.

From these results, we propose a mechanism for methyl migration in **4** in the presence of AN. This involves two pathways (Scheme 1): one is a direct thermolysis from **4** to **8**, and the other an associative pathway via an AN-coordinated intermediate (**9**). A fast equilibrium is assumed to exist between **4** + AN and **9**. According to Scheme 1, the rate of formation of **8** can be expressed as:

$$\begin{aligned} d[\mathbf{8}]/dt &= (k_1 + k_2 K[AN])/(1 + K[AN]) \\ &\quad \times ([Pt]_0 - [\mathbf{8}]) \\ &= k_{obs.}([Pt]_0 - [\mathbf{8}]) \end{aligned} \quad (5)$$

where $[Pt]_0$ is the total concentration of platinum and

$$k_{obs.} = (k_1 + k_2 K[AN])/(1 + K[AN]) \quad (6)$$

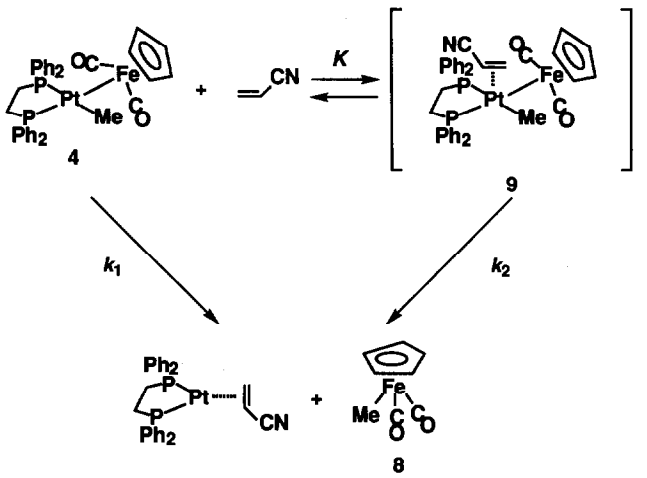

Scheme 1. Proposed mechanism for the methyl migration in 4.

Equation (6) agrees well with Fig. 4 derived from the experimental results. We suggest that the contribution of K in eqn. (6) is sufficiently large to give the curves shown in Fig. 4. It is likely that the reductive elimination of **8** from **9** is accelerated by a decrease in the electron density of Pt, resulting from an increase in the back-bonding from Pt to AN.

In Fig. 4, the value of $k_{obs.}$ at [olefin] = 0 corresponds to the rate constant for thermolysis (k_1). Note that in Fig. 4 the concentration of **4** is of the order of four or five times smaller than that of the olefin (see also Table 5). Thus, the curves in Fig. 4 show that direct thermolysis is more effective than the associative pathway at molar ratios of [olefin] up **4** up to *ca.* 100. In addition, Fig. 4 and eqn. (6) imply that the k_2 values for the three olefins become constant at larger concentrations of olefin. Since k_2 is larger than k_1, this implies that reductive elimination from **9** to **8** is greater than direct thermolysis.

In summary, a series of Pt-containing heterodinuclear complexes with methyl and 1,2-bis(diphenylphosphino)ethane (dpe) ligands has been prepared. These complexes have been characterized by IR and NMR spectroscopy, elemental analysis and chemical reactions, and the structure of (dpe)MePt–FeCp(CO)$_2$ has been determined by X-ray crystallography. The new complexes are more stable thermally than their cod analogues, but the Pt–Fe complex undergoes methyl migration on thermolysis at 70°C to give MeFeCp(CO)$_2$. Such methyl migration is accelerated by CO and olefins, e.g. acrylonitrile and fumaronitrile. Kinetic investigation of the migration has been performed and a reaction mechanism is proposed.

3. Experimental details

3.1. General

All manipulations were carried out under a nitrogen or argon atmosphere using standard Schlenk techniques [6,16]. Solvents were dried over and distilled from appropriate drying agents under N_2: hexane, benzene, toluene, diethyl ether and THF from Na/benzophenone ketyl; CH_2Cl_2 from P_2O_5. Acrylonitrile and vinyl acetate were dried over $CaCl_2$ and vacuum-distilled under N_2. Fumaronitrile was used as received. NMR solvents were freeze–pump–thaw degassed and vacuum-transferred from appropriate drying agents (C_6D_6 from Na; $CDCl_3$ from P_2O_5). PtMeCl(dpe) [17], Na[MoCp(CO)$_3$] [18], Na[WCp(CO)$_3$] [18], Na[FeCp(CO)$_2$] [19], Na[Co(CO)$_4$] [20] and Na[Mn(CO)$_5$] [21] were synthesized according to literature methods. NMR spectra were obtained on a JEOL FX-200 spectrometer (^{1}H, 199.5 MHz). IR spectra were measured in a JASCO FT–IR 5M spectrometer. UV–visible spectra were obtained on Hitachi 320A and Shimadzu UV-120-02 spectrophotometers. Elemental analyses were performed with a Yanagimoto CHN Autocorder MT-2. Molar electrical conductivity was measured on a TOA Conduct Meter CM-7B. Gas chromatography was carried out using a Shimadzu GC-8A instrument.

3.2. Synthesis of (dpe)MePt–ML$_n$ (1–5)

A typical procedure for (dpe)MePt–FeCp(CO)$_2$ · THF (**4** · THF) is given. To a THF solution of PtMeCl(dpe) (198.2 mg, 0.308 mmol) was added $AgNO_3$ (52.3 mg, 0.308 mmol). Stirring at room temperature for 2 h gave a colorless solution with a white precipitate of AgCl. To the filtered solution, a THF solution of Na[FeCp(CO)$_2$] prepared *in situ* from [FeCp(CO)$_2$]$_2$ (101.8 mg, 0.288 mmol) and Na/Hg, was added at −30°C and the mixture stirred for 3 h. The resulting solution was evaporated to dryness and the resulting dark red solids extracted with toluene. After the filtered solution was again evaporated to dryness, the solids were extracted with THF and addition of hexane gave red cubic crystals. The crystals were washed with cold hexane and dried under vacuum (146.2 mg); yield, 60%; m.p. 160°C (dec.). Analysis: Calc. for $C_{38}H_{40}O_3P_2FePt$: C, 53.22; H, 4.70%. Found: C, 53.06; H, 4.82%. Molar electric conductivity Λ (in THF at r.t.), 0.012 S cm^2 mol^{-1} UV–vis.: 322 nm (ε = *ca.* 30000 M^{-1} cm^{-1}). IR and ^{1}H NMR: see Table 1.

Other complexes **1–3** and **5** were prepared by similar methods and their yields, melting points, analytical data and molar electric conductivities are given below.

(dpe)MePt–MoCp(CO)$_3$ (**1**): Green–yellow crystals from benzene/hexane; yield, 89%; m.p., 175°C (dec.). Analysis: Calc. for $C_{35}H_{32}O_3P_2MoPt$: C, 49.25; H,

3.78%. Found: C, 49.22; H, 4.03%. Λ (in THF at r.t.), 0.024 S cm^2 mol^{-1}.

(dpe)MePt–WCp(CO)$_3$ (**2**): Yellow crystals from benzene/hexane; yield, 74%; m.p., 207°C (dec.). This complex was identified by spectroscopic methods (see Table 1). Λ (in THF at r.t.), 0.011 S cm^2 mol^{-1}.

(dpe)MePt–Mn(CO)$_5$ (**3**): Orange cubic crystals from benzene/hexane; yield, 79%; m.p., 165°C (dec.). Analysis: Calc. for $C_{32}H_{27}O_5P_2MnPt$: C, 47.83; H, 3.39%. Found: C, 47.11; H, 4.14%. Λ (in THF at r.t.), 0.061 S cm^2 mol^{-1}.

(dpe)MePt–Co(CO)$_4$ (**5**): Orange cubic crystals from benzene/hexane; yield, 93%; m.p., 170°C (dec.). Analysis: Calc. for $C_{31}H_{27}O_4P_2CoPt$: C, 47.76; H, 3.62%. Found: C, 47.07; H, 3.44%. Λ (in THF at r.t.), 0.19 S cm^2 mol^{-1}.

Acidolysis of **1** was performed by the following procedure. Compound **1** (12.2 mg, 0.0137 mmol) was placed in a Schlenk flask fitted with a serum cap and the system was degassed. Conc. H_2SO_4 (100 μl) was added by means of a hypodermic syringe. After 1 h stirring at room temperature, CH_4 (89%) was detected by GC methods. Yields of CH_4 for **2–5**: **2**, 98%; **3**, 80%; **4**, 70%; **5**, 68%.

3.3. X-Ray crystallography of (dpe)MePt–FeCp(CO)$_2$ · THF (4 · THF)

A crystal of a suitable size was sealed in a thin-glass capillary under N_2. The intensity data were collected at room temperature on a Rigaku AFC-5R four-circle diffractometer. The structure was solved and refined using the CRYSTAN program system (Rigaku) with no absorption correction being applied; 8800 unique reflections, of which 6642 ($|F_o| > 3\sigma|F_o|$), were observed. The structure was solved by the direct method and refined by a full matrix least-squares procedure. All the non-hydrogen atoms were refined anisotropically. Hydrogen atoms were included in the calculation, but they were not refined. Final R (R_w) = 0.066 (0.080).

3.4. Iodolysis of 1–5

Iodolysis was performed in NMR sample tubes. Typically, the procedure for **4** is given. C_6D_6 was vacuum-transferred to an NMR sample tube containing **4** (19.5 mg, 0.0248 mmol), and dioxane (1 μl) as internal standard was added to the solution. After the ^{1}H NMR spectrum of the solution had been measured, I_2 (6.3 mg, 0.025 mmol) was added and the reaction was followed by ^{1}H NMR spectroscopy. For the products and their yields, see Table 4.

3.5. Thermolysis of 1–5

C_6D_6 was vacuum-transferred to an NMR sample tube containing **4** (9.6 mg, 0.012 mmol) and dioxane (1 μl) as internal standard was added to the solution. After the ^{1}H NMR spectrum of the solution had been measured, the sample tube was heated for 2 h at 70°C. The tube was cooled to room temperature and the ^{1}H NMR spectrum measured: MeFeCp(CO)$_2$ (30%). No reaction took place with **1–3** and **5** under the same conditions.

3.6. Reaction of 1–5 with CO

Reactions of **1–5** with CO were performed in NMR sample tubes. Typically, the procedure for **4** is given. C_6D_6 was vacuum-transferred to an NMR sample tube containing **4** (10.6 mg, 0.0135 mmol) and dioxane (1 μl) as internal standard was added to the solution. After the ^{1}H NMR spectrum of the solution had been measured, CO gas (1 atm) was introduced. The sample tube was allowed to stand for 3 h at room temperature and the ^{1}H NMR spectrum again measured: **8** (8%), [FeCp(CO)$_2$]$_2$ (trace). Under the same reaction conditions, **3** gave MeMn(CO)$_5$ (11%) and MeCOMn(CO)$_5$ (27%). No reaction took place with **1**, **2** and **5** under the same conditions.

3.7. Reaction of 1–5 with olefins

Reactions of **1–5** with olefins were performed in NMR sample tubes. Typically, the procedure for **4** with acrylonitrile is given. C_6D_6 was vacuum-transferred to an NMR sample tube containing **4** (9.7 mg, 0.012 mmol) and dioxane (1 μl) as internal standard was added to the solution. After the ^{1}H NMR spectrum of the solution had been measured, acrylonitrile (1 μl) was added by means of a hypodermic syringe. The sample tube was allowed to stand for 2 h at room temperature and the ^{1}H NMR spectrum again measured: **8** (26%). After 78 h, the yields of **8** and (dpe)Pt(AN) were 96 and 75%, respectively. No reaction took place with **1–3** and **5** under the same conditions.

The reaction of **3** with acrylonitrile at 50°C was performed as follows. Compound **3** (9.6 mg, 0.012 mmol) was dissolved in C_6D_6 in an NMR sample tube and dioxane (1 μl) and acrylonitrile (1 μl) added to the solution. The sample tube was heated for 1 h at 50°C, then cooled to room temperature and the ^{1}H NMR spectrum again measured: MeMn(CO)$_5$ (17%).

To isolate (dpe)Pt(AN), the following reaction was conducted. To a THF solution of **4** (103.3 mg, 0.132 mmol) was added AN (180 μl, 2.57 mmol). After stirring for 20 h at room temperature, addition of hexane to the solution gave yellow–brown solids. The solids were extracted with THF and addition of hexane gave brown crystals. These crystals were washed with hexane and dried under vacuum (19.8 mg); yield, 23%; m.p., 113°C (dec.). Analysis: Calc. for $C_{29}H_{27}NP_2Pt$: C,

53.87; H, 4.21; N, 2.17%. Found: C, 53.53; H, 4.35; N, 2.22%. IR (KBr) (cm^{-1}); 2198 (CN). ^{1}H NMR (200 MHz, C_6D_6)δ: 6.9–8.0 (m, dpe C_6H_5); 2.4–3.0 (m, 3H, CH_2=CHCN); 1.7–2.2 (m, 4H, dpe CH_2) ppm.

3.8. Kinetic study of methyl migration in 4 in the presence of AN

An optical cell attached to a Schlenk flask was used for measurement of the UV–vis. spectra under a nitrogen atmosphere. To the Schlenk flask containing **4** (0.0001 mmol) was introduced THF (3–5 ml) by vacuum-transfer, the volume of added THF being estimated from the weight. A known amount of AN (10–250 μl) was added to the solution by means of a hypodermic syringe and the concentration of AN precisely calculated. The temperature of the cell was kept constant at 38.0 ± 1.0°C using an EYELA NCB-110 circulator. The reaction was monitored by means of the electronic absorption spectra over the range 250–600 nm and the decrease in the absorbance of the peak at 322 nm was used to calculate $\ln([Pt]_0/([Pt]_0 - [\mathbf{8}]))$. First-order plots of $\ln([Pt]_0/([Pt]_0 - [\mathbf{8}]))$ versus time gave straight lines, the pseudo-first-order rate constants ($k_{obs.}$) being estimated from the slopes.

4. Supplementary materials available

The atomic parameters, temperature factors of the non-hydrogen atoms, bond distances and bond angles, observed and calculated structure factors (25 pages) for the X-ray crystallography of **4** are available from one of the authors (S.K.).

Acknowledgment

This work was supported by a Grant-in-Aid for Scientific Research from the Ministry of Education, Science and Culture, Japan.

References

1 (a) B.F.G. Johnson (ed.), *Transition Metal Clusters*, Wiley, Chichester, 1980; (b) D.W. Stephan, *Coord. Chem. Rev.*, *95* (1989) 41; (c) D.F. Shriver, H.D. Kaesz and R.D. Adams (eds.), *The Chemistry of Metal Cluster Complexes*, VCH Publishers, New York, 1990; (d) B.C. Gates, L. Guczi and H. Knözinger (eds.), *Metal Clusters in Catalysis*, Elsevier, Amsterdam, 1986; (e) G. Süss-Fink and G. Meister, *Adv. Organomet. Chem.*, *35* (1993) 41.

2 (a) S. Komiya and I. Endo, *Chem. Lett.*, (1988) 1709; (b) A. Fukuoka, T. Sadashima, I Endo, N. Ohashi, Y. Kambara, K. Miki, N. Kasai and S. Komiya, *Organometallics*, submitted for publication.

3 A. Fukuoka, N. Ohashi and S. Komiya, *Chem. Lett.*, (1992) 69.

4 K. Miki, N. Kasai, I. Endo and S. Komiya, *Bull. Chem. Soc. Jpn.*, *62* (1989) 4033.

5 M. Ferrer, O. Rossell, M. Seco and P. Braunstein, *J. Chem. Soc., Dalton Trans.*, (1989) 379.

6 A. Yamamoto, *Organotransition Metal Chemistry*, Wiley, New York, 1986.

7 (a) J.E. Ellis and E.A. Flom, *J. Organomet. Chem.*, *99* (1975) 263; (b) M. Akhtar and H.C. Clark, *ibid.*, *22* (1970) 233.

8 H.E. Bryndza, L.K. Fong, R.A. Paciello, W. Tam and J.E. Bercaw, *J. Am. Chem. Soc.*, *109* (1987) 1444.

9 (a) J. Powell, M.R. Gregg and J.F. Sawyer, *J. Chem. Soc., Chem. Commun.*, (1987) 1029; (b) R. Mason, J. Zibieta, A.T.T. Hsieh, J. Knight and M.J. Mays, *ibid.*, (1972) 200; (c) G. Longoni, M. Manassero and M. Sansoni, *J. Am. Chem. Soc.*, *102* (1980) 3242; (d) *idem, ibid.*, *102* (1980) 7973; (e) L.J. Farrugia, J.A.K. Howard, P. Mitrprachachon, F.G.A. Stone and P. Woodward, *J. Chem. Soc., Dalton Trans.*, (1981) 1134.

10 (a) L. Manojlovic-Muir, K.W. Muir, T. Solomun, D.W. Meek and J.L. Peterson, *J. Organomet. Chem.*, *146* (1978) C26; (b) M.R. Snow, J. McDonald, F. Basolo and J. Ibers, *J. Am. Chem. Soc.*, *94* (1972) 2526; (c) M.R. Snow and J. Ibers, *Inorg. Chem.*, *12* (1973) 224; (d) M.A. Bennet, H.-K. Chee and G.B. Robertson, *ibid.*, *18* (1978) 1061.

11 M.R. Churchill and W.Y. Chang, *J. Am. Chem. Soc.*, *95* (1973) 5931.

12 M. Akita, A. Kondoh and Y. Moro-oka, *J. Chem. Soc., Dalton Trans.*, (1989) 1627.

13 K. Tatsumi, R. Hoffman, A. Yamamoto and J.K. Stille, *Bull. Chem. Soc. Jpn.*, *54* (1981) 1857.

14 T. Yamamoto, A. Yamamoto and S. Ikeda, *J. Am. Chem. Soc.*, *93* (1971) 3350.

15 (a) J. Brandrup and E.H. Immergut (eds.), *Polymer Handbook*, 2nd edn., Wiley, New York, 1975; (b) J. Fujikura and T. Tsuruta, *J. Polym. Sci.*, *36* (1959) 257.

16 D.F. Shriver and M.A. Drezdson, *The Manipulation of Air-Sensitive Compounds*, 2nd edn., Wiley, New York, 1986.

17 T.G. Appleton, M.A. Bennet and I.B. Tomkins, *J. Chem. Soc., Dalton Trans.*, (1976) 439.

18 T.S. Piper and G. Wilkinson, *J. Inorg. Nucl. Chem.*, *3* (1956) 104.

19 R.B. King and F.G.A. Stone, *Inorg. Synth.*, *7* (1963) 110.

20 J.K. Ruff and W.J. Schlientz, *Inorg. Synth.*, *15* (1957) 192.

21 R.B. King and F.G.A. Stone, *Inorg. Synth.*, *7* (1963) 198.